

宇佐見俊介^{1,2}、銭谷誠司³、堀内利得¹

Shunsuke USAMI^{1,2}, Seiji ZENITANI³, Ritoku HORIUCHI¹

核融合研¹、東大²、神戸大³、
NIFS¹, Univ. Tokyo², Kobe Univ.³

Magnetic reconnection is a fundamental process which contains various kinetic physics such as acceleration, heating, and chaotic motions. In order to clarify the kinetic physics related to magnetic reconnection, particle velocity distributions are analyzed in simulations and satellite observations.

This work focuses on crescent-shaped velocity distributions. In 2016, crescent-shaped electron distributions have been observed by the MMS satellite [1], and have been investigated by particle simulations [2,3]. In contrast, we deal with ion crescent. Our particle simulations show that ion crescent distributions often coexist with a ring distribution [4-6], as depicted in Fig. 1(a). Note that the crescent of electrons and of ions are formed in completely different situations; electron crescent is formed in asymmetric reconnection with no guide magnetic field, while ion crescent is created in symmetric reconnection with a guide field.

Despite the above situation difference, we successfully apply the framework for electron crescent [2,3] to ion crescent. We consider a quasi-steady 1D reconnection layer along the inflow line (the y direction). The electromagnetic fields are taken to be $B_z(y)$ and $E_y(y)$, and the other components are ignored. The conservation of the canonical momentum and the energy leads to

$$v_x - v_{x0} = -q/m A_x(y), \quad (1)$$

$$(v_{x0}^2 + v_{y0}^2)/2 = (v_x^2 + v_y^2)/2 + q/m \phi(y), \quad (2)$$

where the subscript 0 means quantities in the upstream, and $A_x(y)$ and $\phi(y)$ denote the vector and electrostatic potentials, respectively. From Eqs. (1) and (2), by virtue of $v_{y0}^2 > 0$, we have

$$v_x > \left[\frac{m}{2q} v_y^2 - \frac{q}{2m} A_x^2(y) + \phi(y) \right] / A_x(y), \quad (3)$$

where $A_x < 0$ is assumed. The inequality (3) indicates the inner boundary of crescent distribution at a given position y in the downstream. On the other hand, substituting the maximum $v_{0\max}^2$ into $v_{x0}^2 + v_{y0}^2$ of Eq. (2), the outer boundary is obtained:

$$v_x^2 + v_y^2 < v_{0\max}^2 - 2q/m \phi(y). \quad (4)$$

The boundaries (3) and (4) account for the ion crescent distributions found in our simulations.

Next, let us observe the (v_y, v_z) plane. We

extract ions constituting the crescent from Fig. 1(a) and show the velocity distributions of the ions. A crescent-shaped distribution is seen as well as in the (v_x, v_y) plane. Furthermore, in Fig. 2, we plot ion velocities in the (v_x, v_y, v_z) space. This helps us intuitively grasp a three-dimensional crescent-like structure. Now we are constructing a 3D theory which accounts for 3D crescent-shaped distributions.

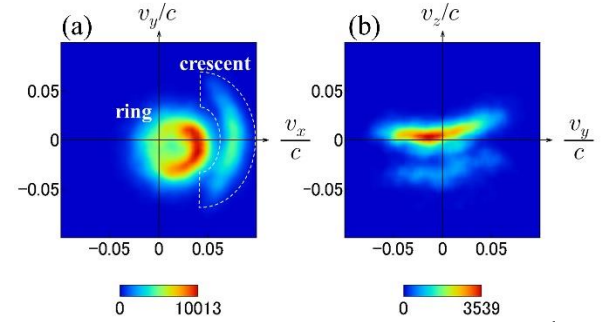


Fig.1: Ion velocity distributions (a) in the (v_x, v_y) plane and (b) in the (v_y, v_z) plane.

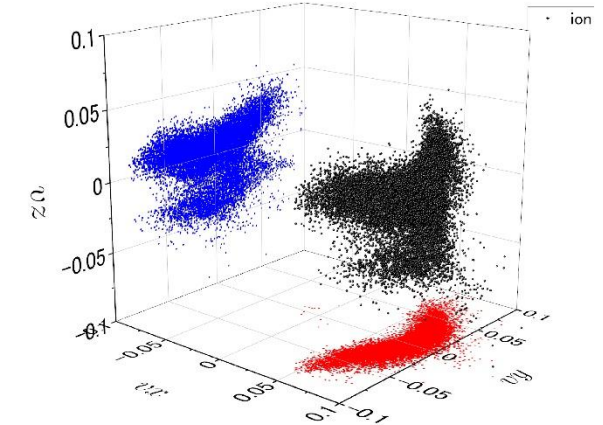


Fig.2: Plots of ion velocities as the black dots. A 3D crescent is seen. The red and blue dots are projections into the (v_x, v_y) and (v_y, v_z) planes, respectively.

References

- [1] J. L. Burch et al., *Science* **352**, aaf2939 (2016).
- [2] N. Bessho et al., *Geophys. Res. Lett.* **43**, 1828, (2016).
- [3] S. Zenitani et al., *J. Geophys. Res. Space Phys.* **112**, 7396 (2017).
- [4] S. Usami et al., *Phys. Plasmas* **24**, 092101 (2017).
- [5] S. Usami et al., *Phys. Plasmas* **26**, 102103 (2019).
- [6] S. Usami and R. Horiuchi, *Front. Astron. Space. Sci.* **9**, 846395 (2022).